Mathematical Biosciences and Engineering

MBE, 21(8): 6807–6828.
DOI: 10.3934/mbe.2024298
Received: 01 May 2024
Revised: 06 July 2024
Accepted: 25 July 2024
Published: 09 August 2024

http://www.aimspress.com/journal/MBE

Research article

Potential for eliminating COVID-19 in Thailand through third-dose vaccination: A modeling approach

Pannathon Kreabkhontho[1], Watchara Teparos[2] and Thitiya Theparod[1,*]

[1] Department of Mathematics, Mahasarakham University, Maha Sarakham 44150, Thailand
[2] Department of General Science, Faculty of Science and Engineering, Kasetsart University, Chalermphrakiat Sakon Nakhon Province Campus, Sakon Nakhon 47000, Thailand

* **Correspondence:** Email: thitiya.t@msu.ac.th.

Abstract: The COVID-19 pandemic continues to pose significant challenges to global public health, necessitating the development of effective vaccination strategies to mitigate disease transmission. In Thailand, the COVID-19 epidemic has undergone multiple waves, prompting the implementation of various control measures, including vaccination campaigns. Understanding the dynamics of disease transmission and the impact of vaccination strategies is crucial for guiding public health interventions and optimizing epidemic control efforts. In this study, we developed a comprehensive mathematical model, termed $SS_vIH_1CH_2RD$, to elucidate the dynamics of the COVID-19 epidemic in Thailand. The model incorporates key epidemiological parameters, vaccination rates, and disease progression stages to assess the effectiveness of different vaccination strategies in curbing disease transmission. Parameter estimation and model fitting were conducted using real-world data from COVID-19 patients in Thailand, enabling the simulation of epidemic scenarios and the exploration of optimal vaccination rates. Our results showed that optimizing vaccination strategies, particularly by administering approximately 119,625 doses per day, can significantly reduce the basic reproduction number (R_0) below 1, thereby accelerating epidemic control. Simulation results demonstrated that the optimal vaccination rate led to a substantial decrease in the number of infections, with the epidemic projected to be completely eradicated from the population by June 19, 2022. These findings underscore the importance of targeted vaccination efforts and proactive public health interventions in mitigating the spread of COVID-19 and minimizing the burden on healthcare systems. Our study provides valuable insights into the optimization of vaccination strategies for epidemic control, offering guidance for policymakers and healthcare authorities in Thailand and beyond. By leveraging mathematical modeling techniques and real-world data, stakeholders can develop evidence-based strategies to

combat the COVID-19 pandemic and safeguard public health.

Keywords: mathematical modeling; control strategy; COVID-19 elimination; third-dose vaccination; basic reproduction number

1. Introduction

Severe acute respiratory syndrome Coronavirus 2 (SARS-CoV-2) is an infectious respiratory disease known as the coronavirus disease 2019 (COVID-19). The outbreak originated in Wuhan, the capital of Hubei Province, People's Republic of China, with the first cases reported in December 2019, initially linked to the Wuhan Seafood Market [1]. Shortly after the first case was identified, the World Health Organization declared the COVID-19 outbreak a global public health emergency [2–5]. As of March 11, 2024, there have been approximately 703,997,824 million confirmed cases of COVID-19, with over 7 million fatalities, with the United States reporting the highest number of infections [6]. Thailand reported its first COVID-19 case on January 31, 2019, which marked the beginning of a steady increase in infections. Thailand has experienced five waves of the epidemic, the most recent of which began in early 2022. As of March 1, 2024, Thailand recorded 34,569 deaths and 4,760,813 confirmed cases [6–8].

Regarding vaccinations, 33,987,074 individuals received the first dose, 53,730,348 received the second dose, and 57,233,919 received the third dose [7–9]. COVID-19 has not been completely eradicated, even though the outbreak's peak has passed throughout the nation. In Thailand, COVID-19 infections are still widespread, and hospitals are still treating patients who require ventilators for severe pneumonia. There has been a decline in the use of self-defense techniques, which has increased the number of cases. Furthermore, a small percentage of the population in Thailand is either unvaccinated or has not completed vaccinations [10].

To curb the spread of COVID-19, Thailand has implemented various measures, including extensive vaccination campaigns, social distancing protocols, frequent cleaning of floors and surfaces, mandatory mask-wearing, and stringent environmental hygiene practices [11]. Vaccination campaigns have proven to be pivotal in preventing infections and mitigating disease severity. Thailand has administered five different types of vaccines: Sinovac, Sinopharm, AstraZeneca, Pfizer, and Moderna vaccines. The vaccination drive commenced on February 28, 2022, with the aim of inoculating the entire population. Facing limited vaccine availability and prevalence of the Delta variant, the Thai government adopted a combined vaccination approach to expedite the immunization process and curb the rising number of infections [12–17]. As a result, Thailand offers a variety of vaccine formulations with varying degrees of efficacy in preventing viral transmission. For instance, the overall infection prevention efficacy of the vaccines was 89% after each dose. Specifically, the vaccine demonstrated 58% effectiveness four weeks after the initial dose, 64% efficacy six months after the second dose, and 44% efficacy six months after the third dose. Within four weeks after the third dose, the efficacy rose to 92%, reaching 88% within two to two-and-a-half months after the third dose, and remained at 83% efficacy two-and-a-half months or more after the third dose [18–22].

The development of epidemic system dynamics models offers robust forecasting techniques and tools for guiding decisions in public health emergency management. These models simulate the disease progression, emergency response strategies, and transmission patterns. They are built upon the

foundation of the SIR epidemic model, which categorizes individuals into susceptible, infected, and recovered compartments [23]. The SIR model or its variations, such as the SIRS [24], SEIR or SEIRD models [25,26], and the SEQIAHR model pioneered by Sacrifice Nana-Kyere [27], have been extensively utilized in simulation studies to illustrate the dynamics of COVID-19. Additionally, more sophisticated compartmental extensions have been explored [28–31].

Mathematical models related to the COVID-19 pandemic are currently being developed to address the ongoing outbreaks. When it comes to vaccination to prevent and control epidemics, these models are incredibly useful in both research and education. They assist in the comprehension and control of various diseases. As a result, many studies have examined the effects of individual immunization doses. For instance, Intawong et al. [32] examined the effects of administering more than three doses of vaccination to high-risk COVID-19 patients in Thailand who have insufficient immunity. Similar research has been undertaken in prior studies [33–38], examining the impact of administering all three immunization doses on the transmission of COVID-19 in various countries. As the government of Thailand endeavors to ensure that its citizens receive all three vaccinations by early 2022, this proactive measure is expected to substantially diminish the probability of contracting infections that might undergo further mutations. Moreover, if infections occur, their severity is anticipated to be reduced, thereby mitigating hospitalization and mortality rates. Recently, Theparod et al. [39] studied the impact of booster dose vaccinations on the recent COVID-19 wave in Thailand. Their findings revealed a dose-dependent decrease in the percentage of infected individuals among the vaccinated population, with the simulation results closely aligned with real-world data. Notably, individuals who received vaccinations exhibited a better recovery rate, while those who received booster doses had the lowest mortality rate. These findings align with previous research [40] affirming the efficacy of administering three vaccine doses in conferring protection against COVID-19, thereby reducing disease severity and mitigating mortality rates as well as infection rates. However, individuals with compromised immune systems, particularly healthcare professionals, necessitate additional vaccine doses. Therefore, it is interesting to explore the impact of implementing a third-dose policy on controlling COVID-19 spread with the aim of eliminating COVID-19 in the population.

In this study, we introduce a comprehensive mathematical model delineating the dynamics of the COVID-19 pandemic, denoted as $SS_vIH_1CH_2RD$. Our study was motivated by the work of Theparod et al. [39], wherein we refined the model to incorporate recent data updates and insights into the disease transmission dynamics. Our model accounts for the recovery trajectory following intensive care unit (ICU) treatment. Given the established efficacy of the third dose in curbing disease transmission, we aim to explore the potential impact of the third-dose strategy on disease elimination. Specifically, this study endeavors to utilize the developed mathematical model to assess the effects of administering a third vaccine dose to reduce infection rates and hasten the time until the epidemic is eliminated. Through this investigation, we aim to provide valuable insights into the optimization of vaccination strategies in evolving pandemic scenarios.

The remainder of this study is structured as follows: In the Materials and methods section, we develop a COVID-19 model with a mathematical formulation. The mathematical analysis of the model, including the positive and boundness of the solution, the basic reproduction number, and endemic equilibrium, are presented. The corresponding model parameters are estimated and tabulated in the Model fitting and parameter estimation section. The Results section explores the sensitivity analysis and simulation of the epidemic scenarios. Finally, discussion and conclusion are presented at the end of this paper.

2. Materials and methods

In this study, we present an eight-deterministic compartmental model of COVID-19 that classifies individuals based on their infection status, vaccination status, and hospitalization stages. This model is an adaptation of a previously developed compartmental model [39] with the inclusion of a compartment of the recuperated population after ICU treatment. The total population is represented by $N(t)$ and is divided into 8 compartments: proportion of the susceptible population (S), proportion of the susceptible who have already received the third-dose vaccination (S_v), proportion of the infectious population under home quarantine and self-care (I), proportion of the hospitalized population (H_1), proportion of the critically infected population treated in the ICU (C), proportion of the recuperated population after treatment in the ICU (H_2), proportion of the recovered population (R), and proportion of the dead population (D). Thus, the total population can be expressed as follows:

$$N(t) = S(t) + S_v(t) + I(t) + H_1(t) + C(t) + H_2(t) + D(t) + R(t).$$

The assumptions for this model are as follows:

(i) We assume homogeneous mixing within the population, indicating that each individual in the community has an equal likelihood of interacting with others and acquiring infections when they come into contact;

(ii) We consider unvaccinated, vaccinated with one dose, and vaccinated with two doses populations in the susceptible compartment (S). Therefore, we refer to these individuals as susceptible individuals;

(iii) A vaccinated individual is assumed to be susceptible with a probability of becoming infected once in contact with an infectious person [41];

(iv) The second vaccination dose was administered to more than 90 percent of patients who received the first dose [42]. As a result, the recipient's immunity was boosted immediately following the injection. Therefore, we assume that the effectiveness of the vaccine remains stable over time without any noticeable decline;

(v) The COVID-19 vaccine is not infallible as its efficacy is not 100%. As a result, breakthrough infections can still occur in vaccinated individuals. The level of protection provided by the vaccine may vary depending on the efficacy of each dose.

In our epidemiological model, the progression of individuals through various stages of susceptibility, infection, hospitalization, and recovery from COVID-19 is governed by several key factors. Susceptible individuals face two primary possibilities: Infection, which happens upon contact with an infected individual at a rate denoted by β, or vaccination, received at a rate τ. The efficacy of the vaccine against infection is quantified by $\beta(1 - m_I)$, where m_I represents the vaccine efficacy in preventing infection. Infected individuals may develop more severe symptoms and move to the hospital at a rate ω. Infected individuals can also move to the death compartment at a rate λ. The remaining infected individuals move to the recovery compartment at a rate of γ. Hospitalized individuals may progress to critical condition at a rate α, or face mortality at a rate π. Additionally, those in critical condition may recover enough to leave the ICU at a rate δ, or face mortality at a rate ρ. Post-ICU recovery occurs at a rate of η for individuals treated in the ICU (classified as H_2). The schematic diagram illustrating the constructed model, based on the aforementioned assumptions, can be found in Figure 1.

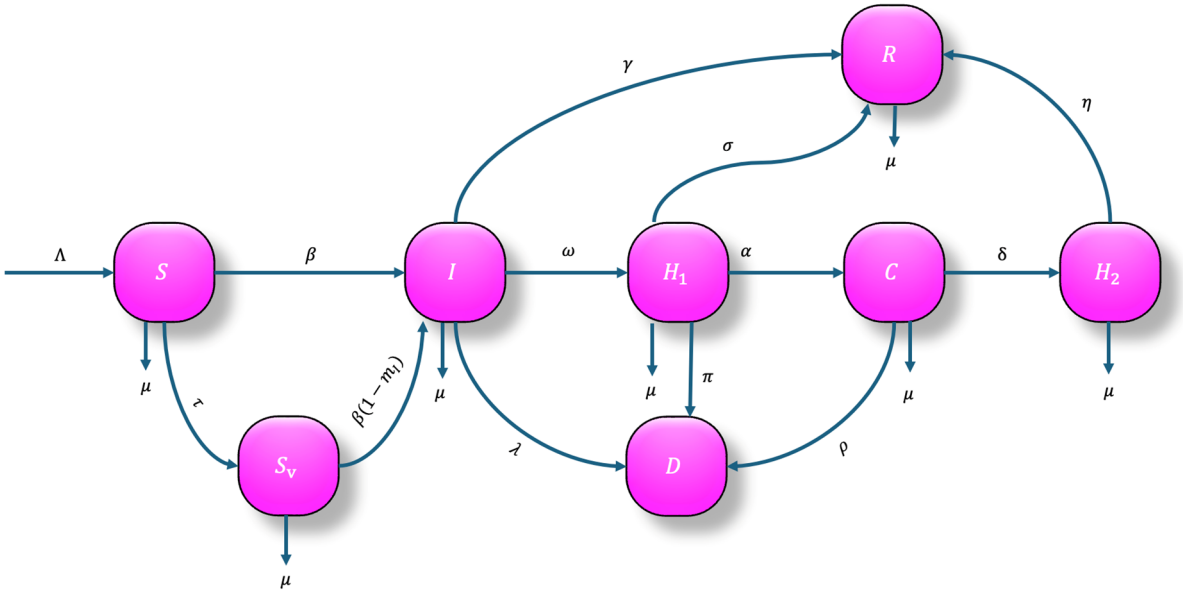

Figure 1. Schematic diagram of the model for disease transmission.

Consequently, the dynamics of COVID-19 are described by the following system of differential equations:

$$\begin{cases} \frac{dS(t)}{dt} = \Lambda - \tau S(t) - \mu S(t) - \beta S(t) I(t) \\ \frac{dS_v(t)}{dt} = \tau S(t) - \mu S_v(t) - \beta(1 - m_I) S_v(t) I(t) \\ \frac{dI(t)}{dt} = \beta S(t) I(t) + \beta(1 - m_I) S_v(t) I(t) - (\lambda + \omega + \gamma + \mu) I(t) \\ \frac{dH_1(t)}{dt} = \omega I(t) - (\pi + \alpha + \sigma + \mu) H_1(t) \\ \frac{dC(t)}{dt} = \alpha H_1(t) - (\rho + \delta + \mu) C(t) \\ \frac{dH_2(t)}{dt} = \delta C(t) - (\eta + \mu) H_2(t) \\ \frac{dR(t)}{dt} = \gamma I(t) + \sigma H_1(t) + \eta H_2(t) - \mu R(t) \\ \frac{dD(t)}{dt} = \lambda I(t) + \pi H_1(t) + \rho C(t) \end{cases} \tag{1}$$

The corresponding initial conditions are:

$$S(0) \geq 0, S_v(0) \geq 0, I(0) \geq 0, H_1(0) \geq 0, C(0) \geq 0, H_2(0) \geq 0, D(0) \geq 0, R(0) \geq 0 \tag{2}$$

Furthermore, Tables 1 and 2 detail all of the state variables and parameters, along with their corresponding descriptions, respectively.

Table 1. State variables and their descriptions.

Variable	Description
S	The proportion of the susceptible population
S_v	The proportion of the susceptible and vaccinated population
I	The proportion of the infectious population under home quarantine and self-care
H_1	The proportion of the hospitalized population
C	The proportion of the critically infected population who are treated in the ICU
H_2	The proportion of the recuperated population after treatment in the ICU
R	The proportion of the recovered population

Table 2. Summary of model parameters and descriptions.

Parameters	Description
Λ	Recruitment rate
μ	Natural death rate
τ	Vaccination rate
β	The effective transmission rate
γ	Recovery from infection
σ	Recovery from infection while in hospital
η	Recovery from recuperation after treatment in the ICU
δ	The recovery rate from infection in the ICU, returning to the recuperation
ω	Hospital admission rate
λ	The death rate of the infected population
π	The death rate of the hospitalized population
ρ	The death rate of the population admitted to the ICU
α	ICU admission rate of infected hospitalized individuals
m_I	The efficacy of vaccines for preventing infection

2.1. Data

Data pertaining to COVID-19 were obtained from the COVID-19 Data Repository managed by the Department of Disease Control (DDC) [7]. This repository contains a wide array of information, including daily COVID-19 case counts, hospital admissions, critical cases, recoveries following ICU treatment, daily mortality rates, and vaccination statistics.

Figure 2 illustrates the incidence of COVID-19 from the onset of the pandemic up until the fifth wave. As we can see, a considerable number of cases were reported during the fifth wave of the epidemic, with the highest infection rates compared to the previous waves. Furthermore, in February 2021, Thailand initiated its COVID-19 vaccination campaign with procurement of the Sinovac vaccine from China [43]. As the alpha variant began to spread in March, Thailand expanded its vaccine arsenal by importing the AstraZeneca vaccine from England and Sweden. In June 2021, the country imported the Sinopharm vaccine from China, followed by the introduction of the Pfizer vaccine from Germany in August 2021. Responding to the rise of the delta variant, Thailand commenced administering the Moderna vaccine from the United States in November 2021 [44].

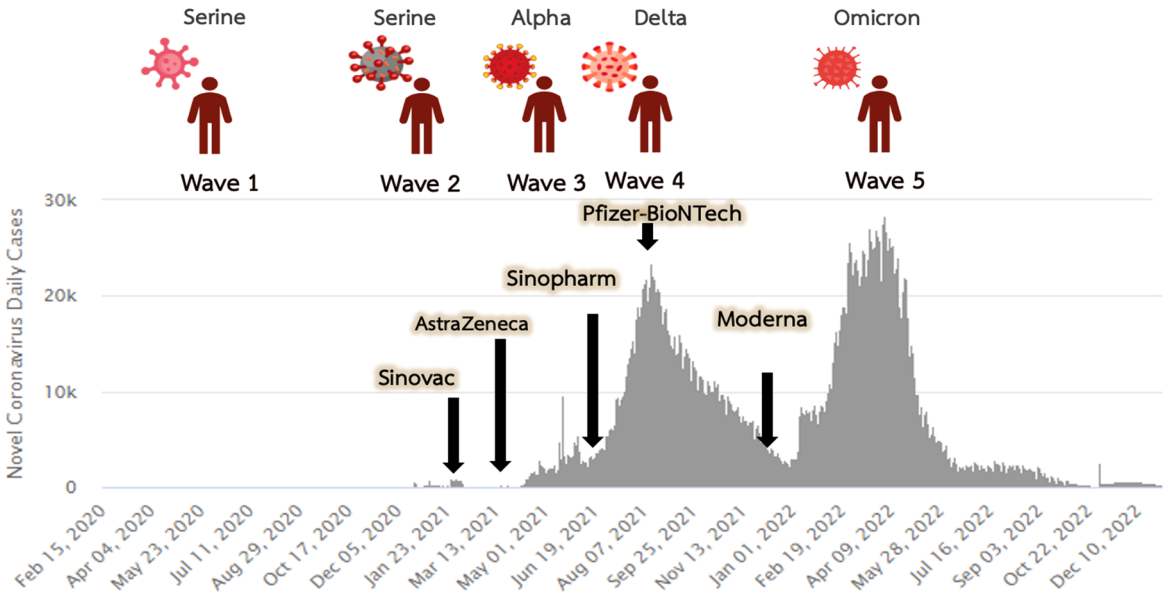

Figure 2. The course of COVID-19 in Thailand from the beginning of the pandemic.

2.2. Positivity and boundedness of the solution

For model (1), a region of attraction is given by Lemma 2.2.

Lemma 2.2. *Set* $\Omega = \{(S, S_v, I, H_1, C, H_2, R, D) \in \mathbb{R}_+^8 : N = S + S_v + I + H_1 + C + H_2 + D + R\}$ *is the invariant region of model (1).*

Proof. Let $N = S + S_v + I + H_1 + C + H_2 + D + R$,and then

$$\frac{dN}{dt} = \frac{dS}{dt} + \frac{dS_v}{dt} + \frac{dI}{dt} + \frac{dH_1}{dt} + \frac{dC}{dt} + \frac{dH_2}{dt} + \frac{dR}{dt} + \frac{dD}{dt},$$

$$\frac{dN}{dt} = \Lambda - \mu N.$$

Integrating $N(t) \leq 1 + (N(0) - 1)e^{-\mu t}$, then $N(t) \leq 1$ and $e^{-\mu t} \to 0$ as $t \to \infty$. This indicates that the solution of model (1) remains non-negative and bounded.

2.3. The basic reproduction number (R_0)

The reproduction number is the average number of secondary infections produced by one infected individual in a completely susceptible population. To compute the basic reproduction number, we use the next-generation approach described by Dietz [45]. Let X = $(I, H_1, C, H_2)^T$ be a vector of infected classes. F represents the Jacobian matrix of the terms that cause new infections and the matrix of the remaining transfer terms is represented as V. The Jacobian matrices, F and V, evaluated at the disease-free equilibrium, are obtained as

$$F = \begin{bmatrix} \beta S + \beta(1 - m_I)S_v & 0 & 0 & 0 \\ 0 & 0 & 0 & 0 \\ 0 & 0 & 0 & 0 \\ 0 & 0 & 0 & 0 \end{bmatrix},$$

$$V = \begin{bmatrix} \lambda+\omega+\gamma+\mu & 0 & 0 & 0 \\ -\omega & \pi+\alpha+\sigma+\mu & 0 & 0 \\ 0 & -\alpha & \rho+\delta+\mu & 0 \\ 0 & 0 & -\delta & \eta+\mu \end{bmatrix}.$$

The next generation matrix is the production of FV^{-1}. The eigenvalues of FV^{-1} are $\Phi_1 = \frac{\beta S+\beta(1-m_I)S_v}{\lambda+\omega+\gamma+\mu}$, $\Phi_2 = 0, \Phi_3 = 0,$ and $\Phi_4 = 0$.

Hence, $R_0 = \rho(FV^{-1}) = max\{|\Phi_1|, |\Phi_2|, |\Phi_3|, |\Phi_4|\} = \frac{\beta\Lambda\mu+\tau\Lambda\beta(1-m_I)}{(\lambda+\omega+\gamma+\mu)\mu(\tau+\mu)}$.

Understanding the basic reproduction number (R_0) is paramount in epidemiological theory for predicting the fate of infectious diseases within populations. When $R_0 < 1$, the disease is destined to extinguish naturally, whereas an $R_0 > 1$ signifies the persistence of the disease within the population for a significant duration. Effective control measures necessitate reducing R_0 below unity. Thus, comprehending the influence of model parameters on the basic reproduction number is critical.

2.4. Endemic equilibrium

The model has two equilibrium points: disease-free equilibrium (DFE), which occurs when $R_0 < 1$, and endemic equilibrium (EE), which occurs when $R_0 > 1$.

Theorem 2.4. *A disease-free equilibrium state (DFE) of model (1) exists at the point* $E_0 = \left(S_0, S_{v_0}, I_0, H_{1_0}, C_0, H_{2_0}, R_0, D_0\right) = \left(\frac{\Lambda}{(\tau+\mu)}, \frac{\tau\Lambda}{\mu(\tau+\mu)}, 0, 0, 0, 0, 0, 0\right)$ *and the endemic equilibrium point exists at* $E^* = (S^*, S_v^*, I^*, H_1^*, C^*, H_2^*, R^*, D^*)$ *where*

$$S^* = \frac{\Lambda}{\tau+\mu+\beta I^*},$$

$$S_v^* = \frac{\tau\Lambda}{(\tau+\mu+\beta I^*)(\mu+\beta(1-m_I)I^*)},$$

$$I^* = \frac{-B\pm\sqrt{B^2-4AC}}{2A},$$

$$H_1^* = \frac{\omega I^*}{(\pi+\alpha+\sigma+\mu)},$$

$$C^* = \frac{\alpha\omega I^*}{(\pi+\alpha+\sigma+\mu)(\rho+\delta+\mu)},$$

$$H_2^* = \frac{\alpha\omega\delta I^*}{(\eta+\mu)(\pi+\alpha+\sigma+\mu)(\rho+\delta+\mu)},$$

$$R^* = \frac{\gamma I^*}{\mu} + \frac{\sigma\omega I^*}{\mu(\pi+\alpha+\sigma+\mu)} + \frac{\eta\alpha\omega\delta I^*}{\mu\left((\eta+\mu)(\pi+\alpha+\sigma+\mu)(\rho+\delta+\mu)\right)},$$

$$D^* = 1 - (S^* + S_v^* + I^* + H_1^* + C^* + H_2^* + R^*),$$

such that

$$A = (\lambda + \omega + \gamma + \mu)\beta^2(1 - m_I),$$

$$B = \big((\lambda + \omega + \gamma + \mu)(\tau + \mu)\beta(1 - m_I) + \mu\beta\big) - \beta^2\Lambda(1 - m_I),$$

$$C = (\lambda + \omega + \gamma + \mu)(\tau\mu + \mu^2) - \tau\Lambda - \mu\beta\Lambda.$$

Proof. The above expressions are deduced by equating all derivatives mentioned in the system of Eq (1) to zero.

We get

$$0 = \Lambda - \tau S(t) - \mu S(t) - \beta S(t)I(t) \tag{3}$$

$$0 = \tau S(t) - \mu S_v(t) - \beta(1 - m_I)S_v(t)I(t) \tag{4}$$

$$0 = \beta S(t)I(t) + \beta(1 - m_I)S_v(t)I(t) - (\lambda + \omega + \gamma + \mu)I(t) \tag{5}$$

$$0 = \omega I(t) - (\pi + \alpha + \sigma + \mu)H_1(t) \tag{6}$$

$$0 = \alpha H_1(t) - (\rho + \delta + \mu)C(t) \tag{7}$$

$$0 = \delta C(t) - (\eta + \mu)H_2(t) \tag{8}$$

$$0 = \gamma I(t) + \sigma H_1(t) + \eta H_2(t) - \mu R(t) \tag{9}$$

$$0 = \lambda I(t) + \pi H_1(t) + \rho C(t) \tag{10}$$

At the disease-free equilibrium state (E_0), all infectious stages are 0, and we have

$$S(t) = S_0,\ S_v(t) = S_{v_0}, I(t) = 0, H_1(t) = 0, C(t) = 0, H_2(t) = 0, R(t) = 0, D(t) = 0.$$

From Eq (3), we get $0 = \Lambda - \tau S(t) - \mu S(t)$, then $S_0 = \frac{\Lambda}{(\tau+\mu)}$. From Eq (3), we have $0 = \tau S(t) - \mu S_v(t)$, then $S_{v_0} = \frac{\tau\Lambda}{\mu(\tau+\mu)}$. Therefore, $E_0 = \big(S_0, S_{v_0}, I_0, H_{1_0}, C_0, H_{2_0}, R_0, D_0\big) = \Big(\frac{\Lambda}{(\tau+\mu)}, \frac{\tau\Lambda}{\mu(\tau+\mu)}, 0,0,0,0,0\Big)$.

Next, we will determine E^*. From (3), we have

$$S^* = \frac{\Lambda}{\tau+\mu+\beta I^*}. \tag{11}$$

From (4), we get $\mu S_v - \beta(1 - m_I)S_v I^* = \tau S$. Then

$$S_v^* = \frac{\tau S^*}{\mu+\beta(1-m_I)I^*} = \frac{\tau\Lambda}{(\tau+\mu+\beta I^*)(\mu+\beta(1-m_I)I^*)}. \tag{12}$$

Substitute (11) and (12) in (5) and since $I^* > 0$, we get

$$0 = \frac{\beta\Lambda}{\tau+\mu+\beta I^*} + \frac{\beta(1-m_I)\tau\Lambda}{(\mu+\beta(1-m_I)I^*)(\tau+\mu+\beta I^*)} - (\lambda + \omega + \gamma + \mu).$$

Let $K = \lambda + \omega + \gamma + \mu$ and, from the above expression, we have

$$0 = \frac{\beta\Lambda(\mu+\beta(1-m_I)I^*)}{(\tau+\mu+\beta I^*)(\mu+\beta(1-m_I)I^*)} + \frac{\beta(1-m_I)\tau\Lambda}{(\tau+\mu+\beta I^*)(\mu+\beta(1-m_I)I^*)} - \frac{K(\tau+\mu+\beta I^*)(\mu+\beta(1-m_I)I^*)}{(\tau+\mu+\beta I^*)(\mu+\beta(1-m_I)I^*)},$$

$$0 = \frac{\beta\Lambda(\mu+\beta(1-m_I)I^*)+\beta(1-m_I)\tau\Lambda-K(\tau+\mu+\beta I^*)(\mu+\beta(1-m_I)I^*)}{(\tau+\mu+\beta I^*)(\mu+\beta(1-m_I)I^*)}.$$

We will obtain the condition of the denominator that $(\tau + \mu + \beta I^*)(\mu + \beta(1 - m_I)I^*) > 0$. Let us look at the numerator.

$$0 = \beta\Lambda(\mu + \beta(1 - m_I)I^*) + \beta(1 - m_I)\tau\Lambda - K(\tau + \mu + \beta I^*)(\mu + \beta(1 - m_I)I^*).$$

We then obtain

$$0 = K\beta^2(1 - m_I){I^*}^2 - \big(K(\tau + \mu)\beta(1 - m_I) + K\mu\beta - \beta^2\Lambda(1 - m_I)\big)I^* - (K\tau\mu - \beta(1 - m_I)\tau\Lambda + K\mu^2 - \mu\beta\Lambda).$$

Let $A = K\beta^2(1 - m_I), B = -\big(K(\tau + \mu)\beta(1 - m_I) + K\mu\beta - \beta^2\Lambda(1 - m_I)\big)$, and $C = -(K\tau\mu - \beta(1 - m_I)\tau\Lambda + K\mu^2 - \mu\beta\Lambda)$. Then, $0 = A{I^*}^2 + BI^* + C$.

Under the condition $B^2 - 4AC \geq 0$, the solutions of this quadratic equation are

$$I^* = \frac{-B \pm \sqrt{B^2 - 4AC}}{2A}. \tag{13}$$

We can see that if $C \leq 0$, the condition $B^2 - 4AC \geq 0$ is true. Consider $\mathrm{C} \leq 0$, we have $K\tau\mu - \beta(1 - m_I)\tau\Lambda + K\mu^2 - \mu\beta\Lambda \leq 0$. Hence $K\tau\mu - \beta(1 - m_I)\tau\Lambda + K\mu^2 - \mu\beta\Lambda \geq 0$, then $K \geq \frac{\beta(1-m_I)\tau\Lambda+\mu\beta\Lambda}{\mu(\tau+\mu)}$.

By substituting I^* in (6)–(9), we get

$$H_1^* = \frac{\omega I^*(t)}{(\pi+\alpha+\sigma+\mu)}, \tag{14}$$

$$C^* = \frac{\alpha\omega I^*(t)}{(\pi+\alpha+\sigma+\mu)(\rho+\delta+\mu)}, \tag{15}$$

$$H_2^* = \frac{\alpha\omega\delta I^*(t)}{(\eta+\mu)(\pi+\alpha+\sigma+\mu)(\rho+\delta+\mu)}, \tag{16}$$

$$R^* = \frac{\gamma I^*(t)}{\mu} + \frac{\sigma\omega I^*(t)}{\mu(\pi+\alpha+\sigma+\mu)} + \frac{\eta\alpha\omega\delta I^*(t)}{\mu\big((\eta+\mu)(\pi+\alpha+\sigma+\mu)(\rho+\delta+\mu)\big)}. \tag{17}$$

2.5. Stability analysis

Initially, we performed a stability analysis at the disease-free and endemic equilibrium points. The results are as follows:

Theorem 2.5.1. *The disease-free equilibrium point, E_0, is stable if $R_0 < 1$, and E_0 is unstable if $R_0 > 1$.*

Proof. The Jacobian matrix of model (1) evaluated at E_0 is

$$J_{E_0}=\begin{bmatrix} -\mu-\tau & 0 & -\beta S_0 & 0 & 0 & 0 & 0 \\ \tau & -\mu & -\beta(1-m_I)S_{v_0} & 0 & 0 & 0 & 0 \\ 0 & 0 & \beta S_0+\beta(1-m_I)S_{v_0}-(\omega+\lambda+\gamma+\mu) & 0 & 0 & 0 & 0 \\ 0 & 0 & \omega & -\alpha-\pi-\mu-\sigma & 0 & 0 & 0 \\ 0 & 0 & 0 & \alpha & -\rho-\delta-\mu & 0 & 0 \\ 0 & 0 & 0 & 0 & \delta & -\eta-\mu & 0 \\ 0 & 0 & \gamma & \sigma & 0 & \eta & -\mu \end{bmatrix}.$$

The characteristic polynomial is $det(J_{E_0}-\phi I_7)=0$. Hence,

$$\det\left(J_{E_0}-\phi I_7\right)=(-\mu-\tau-\phi_1)(-\mu-\phi_2)(\beta S_0+\beta(1-m_I)S_{v_0}-(\omega+\lambda+\gamma+\mu+\phi_3),$$

$$(-\alpha-\pi-\mu-\sigma-\phi_4)(-\rho-\delta-\mu-\phi_5)(-\eta-\mu-\phi_6)(-\mu-\phi_7)=0.$$

We get $\phi_1=-\mu-\tau<0$, $\phi_2=-\mu<0, \phi_4=-\alpha-\pi-\mu-\sigma<0$, $\phi_5=-\rho-\delta-\mu<0$, $\phi_6=-\eta-\mu<0$, and $\phi_7=-\mu<0$.

That is, $\phi_1,\phi_2,\phi_4,\phi_5,\phi_6$, and ϕ_7 are all negative. Considering ϕ_3, $\beta S_0+\beta(1-m_I)S_{v_0}-\omega-\lambda-\gamma-\mu-\phi_3=0$. By substituting S_0 and S_{v_0}, we obtain $\phi_3=\frac{1}{\mu(\tau+\mu)}(\mu\beta\Lambda+\beta(1-m_I)\tau\Lambda-(\omega+\lambda+\gamma+\mu)\mu(\tau+\mu))$.

Since $R_0<1$, then $\beta\Lambda\mu+\tau\Lambda\beta(1-m_I)-(\lambda+\omega+\gamma+\mu)\mu(\tau+\mu))<0$. Therefore, $\phi_3=\frac{1}{\mu(\tau+\mu)}(\mu\beta\Lambda+\beta(1-m_I)\tau\Lambda-(\omega+\lambda+\gamma+\mu)\mu(\tau+\mu))<0$. All eigenvalues are negative. Hence, E_0 is stable.

Theorem 2.5.2. *The endemic equilibrium point, E^*, of model (1) is stable if $R_0>1$ where E^* of the model (1) is stable under the condition that $S^*+(1-m_I)S_v^*\leq\frac{\omega+\lambda+\gamma+\mu}{\beta}$.*

Proof. The mathematical expression of the eigenvalues of the Jacobian matrix of model (1) is tedious. The Jacobian matrix of model (1) evaluated at E^* is

$$J_{E^*}=\begin{bmatrix} -I^*\beta-\mu-\tau & 0 & -\beta S^* & 0 & 0 & 0 & 0 \\ \tau & -\mu-\beta(1-m_I)I^* & -\beta(1-m_I)S_v^* & 0 & 0 & 0 & 0 \\ \beta I^* & \beta(1-m_I)I^* & \beta S^*+\beta(1-m_I)S_v^*-\omega-\lambda-\gamma-\mu & 0 & 0 & 0 & 0 \\ 0 & 0 & \omega & -\alpha-\pi-\mu-\sigma & 0 & 0 & 0 \\ 0 & 0 & 0 & \alpha & -\rho-\delta-\mu & 0 & 0 \\ 0 & 0 & 0 & 0 & \delta & -\eta-\mu & 0 \\ 0 & 0 & \gamma & \sigma & 0 & \eta & -\mu \end{bmatrix}.$$

We have that

$$\det(J_{E^*}-\phi I_7)=(-\alpha-\pi-\mu-\sigma-\phi_4)(-\rho-\delta-\mu-\phi_5)(-\eta-\mu-\phi_6)(-\mu-\phi_7)(-1)(\phi^3+Z_1\phi^2+Z_2\phi+Z_3)=0,$$

where

$$Z_1=(I^*\beta+\mu+\tau)+(\mu+\beta(1-m_I)I^*)-(\beta S^*+\beta(1-m_I)S_v^*-\omega-\lambda-\gamma-\mu),$$

$$Z_2=(I^*\beta+\mu+\tau)(\mu+\beta(1-m_I)I^*)-(I^*\beta+\mu+\tau)(\beta S^*+\beta(1-m_I)S_v^*-\omega-\lambda-\gamma-\mu)+(\beta I^*)(\beta S^*)-(\mu+\beta(1-m_I)I^*)(\beta S^*+\beta(1-m_I)S_v^*-\omega-\lambda-\gamma-\mu)+(\beta(1-m_I)I^*)(\beta(1-m_I)S_v^*),$$

$Z_3 = (I^*\beta + \mu + \tau)(\beta(1-m_I)I^*)(\beta(1-m_I)S_v^*) + (\beta I^*)(\beta S^*)(\mu + \beta(1-m_I)I^*) - (I^*\beta + \mu + \tau)(\mu + \beta(1-m_I)I^*)(\beta S^* + \beta(1-m_I)S_v^* - \omega - \lambda - \gamma - \mu) + (\tau)(\beta S^*)(\beta(1-m_I)I^*)$.

Consider each term in $\det(J_{E^*} - \phi I_7)$, and we have that $\phi_4, \phi_5, \phi_6,$ and ϕ_7 are all negative. According to the Routh–Hurwitz criteria, we need to show that $Z_1 > 0, Z_3 > 0$, and $Z_1 Z_2 > Z_3$ so that the solution of the polynomial has negative real parts. By assumption, $S^* + (1-m_I)S_v^* \leq \frac{\omega+\lambda+\gamma+\mu}{\beta}$. Hence,

$$\beta S^* + \beta(1-m_I)S_v^* - \omega - \lambda - \gamma - \mu \leq 0. \tag{18}$$

Note that (18) is a second term of Z_1. Therefore, it is obvious that $Z_1 > 0$. Now consider Z_3, and we can see that the first, second, and fourth terms of Z_3 are positive. Since (18) is negative, this makes the third term negative. Next, we want to show that $Z_1 Z_2 > Z_3$. Consider the inequality $Z_1 Z_2 - Z_3 > 0$, which is

$(-I^*\beta - \mu - \tau)(\beta I^*)(-\beta S^*) + (\tau)(\beta(1-m_I)I^*)(-\beta S^*) + (-\mu - \beta(1-m_I)I^*)(\beta(1-m_I)I^*)(-\beta(1-m_I)S_v^*) + (\beta(1-m_I)I^*)(-\beta(1-m_I)S_v^*)(\beta S^* + \beta(1-m_I)S_v^* - \omega - \lambda - \gamma - \mu) + (\beta I^*)(-\beta S^*)(\beta S^* + \beta(1-m_I)S_v^* - \omega - \lambda - \gamma - \mu) - (-I^*\beta - \mu - \tau)(-I^*\beta - \mu - \tau)(-\mu - \beta(1-m_I)I^*) - (-I^*\beta - \mu - \tau)(-\mu - \beta(1-m_I)I^*)(-\mu - \beta(1-m_I)I^*) - (-I^*\beta - \mu - \tau)(-I^*\beta - \mu - \tau)(\beta S^* + \beta(1-m_I)S_v^* - \omega - \lambda - \gamma - \mu) - (-\mu - \beta(1-m_I)I^*)(-\mu - \beta(1-m_I)I^*)(\beta S^* + \beta(1-m_I)S_v^* - \omega - \lambda - \gamma - \mu) - (-I^*\beta - \mu - \tau)(\beta S^* + \beta(1-m_I)S_v^* - \omega - \lambda - \gamma - \mu)(\beta S^* + \beta(1-m_I)S_v^* - \omega - \lambda - \gamma - \mu) - (-\mu - \beta(1-m_I)I^*)(\beta S^* + \beta(1-m_I)S_v^* - \omega - \lambda - \gamma - \mu)(\beta S^* + \beta(1-m_I)S_v^* - \omega - \lambda - \gamma - \mu) - (-I^*\beta - \mu - \tau)(-\mu - \beta(1-m_I)I^*)(\beta S^* + \beta(1-m_I)S_v^* - \omega - \lambda - \gamma - \mu) - (-I^*\beta - \mu - \tau)(-\mu - \beta(1-m_I)I^*)(\beta S^* + \beta(1-m_I)S_v^* - \omega - \lambda - \gamma - \mu) > 0.$ (19)

We will show that (19) is true. First, we investigate whether the sum of the first term and the second term is positive. Simplifying the first and the second terms, we have the term $\big((-I^*\beta - \mu - \tau) + \tau(1-m_I)\big)(-\beta^2 I^* S^*)$. Therefore, we only need to show that $\tau(1-m_I) + (-\mu - \tau) < I^*\beta$. It is straightforward to see that $\tau(1-m_I) + (-\mu - \tau) = -\tau m_I - \mu < 0$. Since $\beta I^* > 0$, then $\tau(1-m_I) - \mu - \tau < \beta I^*$. This gives $-\beta I^* - \mu - \tau + \tau(1-m_I) < 0$.

Similarly, according to (18), other terms of (19) are positive. Therefore, $Z_1 Z_2 - Z_3 > 0$. As a result, $Z_1 Z_2 > Z_3$. Hence, the theorem is proved.

3. Model fitting and parameter estimation

Parameter estimation is crucial in infectious disease modeling, as it enables the determination of key parameters governing disease spread. Most of the model parameter values are calculated directly from the daily new case reports of each group of individuals, while others are sourced from existing literature. We define the vaccination rate that accounts for the fact that only those who have received the second dose are eligible for the third dose. The initial values for each state variable were obtained corresponding to the first day of the fifth wave (January 3, 2022). The values of initial conditions and the corresponding estimated parameters are presented in Tables 3 and 4.

Table 3. Variables of model parameters.

State variable	Description	Source
S	58,511,326 (people)	[7]
S_v	7,466,139 (people)	[7]
I	2927 (people)	[7]
H_1	15,945 (people)	[7]
C	704 (people)	[7]
H_2	38 (people)	[7]
R	2903 (people)	[7]

Table 4. Model parameter values corresponding to COVID-19 cases in Thailand.

Parameters	Description	Values	Source
Λ	Recruitment rate	0.00090	[46]
μ	Natural death rate	0.00090	[46]
γ	Recovery from infection	0.1	[14]
σ	Recovery from infection while in hospital	0.10497	calculated
η	Recovery from recuperation after treatment in the ICU	1.12820	calculated
δ	The recovery rate from infection in the ICU, returning to the recuperation	5.66015	fitted
ω	Hospital admission rate	0.93542	fitted
π	The death rate of the hospitalized population	0.00075	calculated
ρ	The death rate of the population admitted to the ICU	0.02643	calculated
α	ICU admission rate of infected hospitalized individuals	0.03537	calculated
β	The effective transmission rate	1.23431	fitted
λ	The death rate of the infected population	0.00823	calculated
τ	Vaccination rate	0.00016	[47]
m_I	The efficacy of vaccines for preventing infection	88%	[48]

Here, we estimated β, ω, and δ using a least squares method called the Nelber-Mead method, which was performed in Rstudio with R version 4.4.1. We defined the objective function using the root mean square deviation (RMSE) and searched for parameters that minimized the distance between the actual data points and the predicted values. Our parameter estimation was based on real data from COVID-19 patients confirmed in Thailand from January 3, 2022, until October 31, 2022. Note that Thailand started to report new confirmed cases weekly instead of daily after October 31 because the number of new cases was too small. Moreover, parameters σ, η, π, ρ, α, and λ were calculated using case count data obtained from the Department of Disease Control (DDC). The rates were calculated based on the average number of people moving to each stage per unit of time (day).

With Thailand's total population estimated at approximately 66,000,000, and initial counts of 2927 symptomatic patients, 15,945 hospitalizations, and 704 in the ICU, the initial susceptible population was approximated at 65,960,334. Figure 3 illustrates the incidence data along with the model-fitting curve, depicting the estimated parameter values. The solid blue curve corresponds to the model fit, whereas the dark gray dots represent the observed data points. Additionally, the light and blue-shaded bounds indicate the 95% confidence intervals (CI).

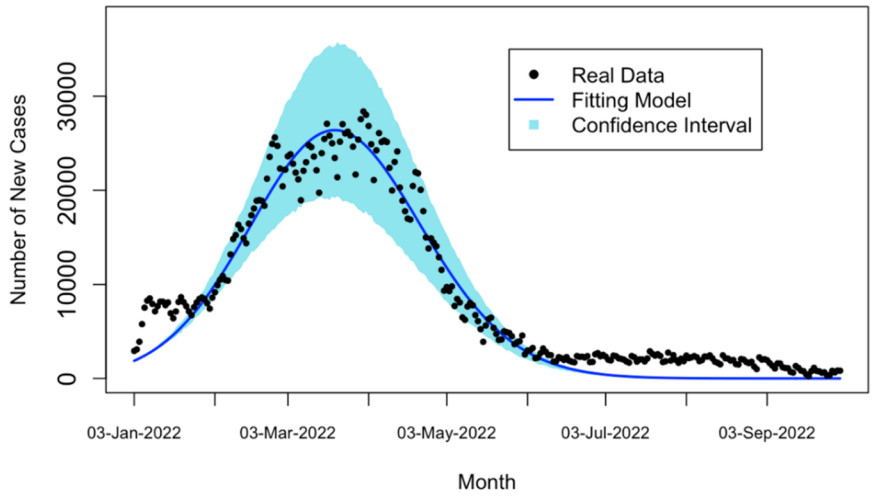

Figure 3. Results of the fitted model compared with data on the number of people infected with COVID-19 with a 95% confidence interval (blue area).

4. Sensitivity analysis

Assessing the impact of model parameters on key epidemiological metrics, such as the basic reproduction number and infected population, is imperative in guiding decision-making for controlling the spread of the disease. This section presents a global sensitivity analysis of the mathematical model (model (1)). To determine the most influential l0 parameters governing the model behavior, we employed Latin hypercube sampling (LHS) and partial rank correlation coefficient (PRCC) techniques [49]. By applying these methods, we identified pivotal factors that demand attention, providing decision-makers with essential insights for formulating a more evidence-based COVID-19 control strategy.

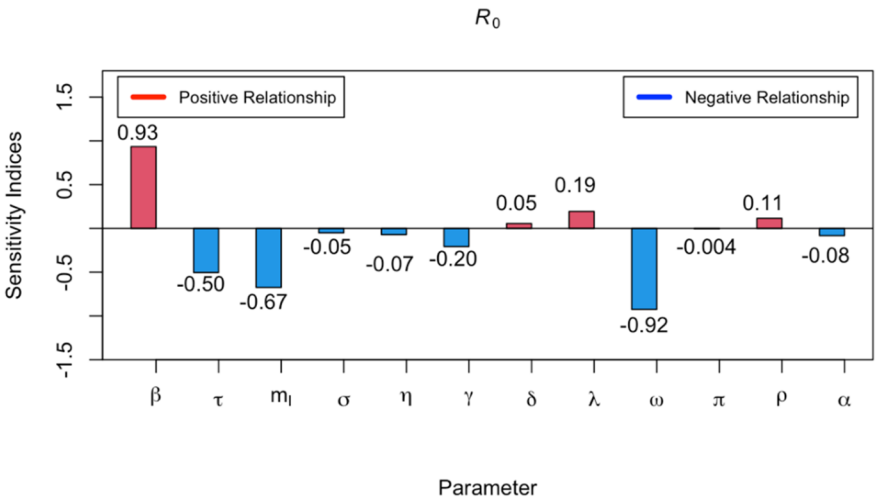

Figure 4. Sensitivity indexes table for the basic reproduction number.

Through computational simulations spanning 1000 days, we performed sensitivity analyses, excluding the recruitment rate of the susceptible class (Λ) and the natural death rate (μ). The outcomes

of this analysis, illustrated in Figure 4, specifically focus on the PRCC concerning the basic reproduction number (R_0). Notably, among the parameters examined, two emerged as significantly influential: the effective transmission rate (β), which has a positive effect on the basic reproduction number (R_0), and the efficacy of the vaccine against infection (m_I) with negative effect on R_0. This implies that a 10% increase or decrease in β will result in a 9.3% increase or decrease in R_0. Whereas, a 10% increase or decrease in m_I will result in a 6.7% decrease or increase in R_0.

Furthermore, we investigate the most influential parameters affecting each infected compartment as depicted in Figure 5. Our findings show that the efficacy of the third dose in preventing infection (m_I) remains the paramount parameter for all compartments, followed by the effective transmission rate (β). The hospital admission rate (ω) and the mortality rate of hospitalized individuals (π) also have a high impact on the hospitalized compartment (H_1), while parameters σ and δ play influential roles in the critical compartment (C). Lastly, for the recuperation compartment (H_2), the mortality rates of hospitalized individuals and patients admitted to the ICU also exert significant impact.

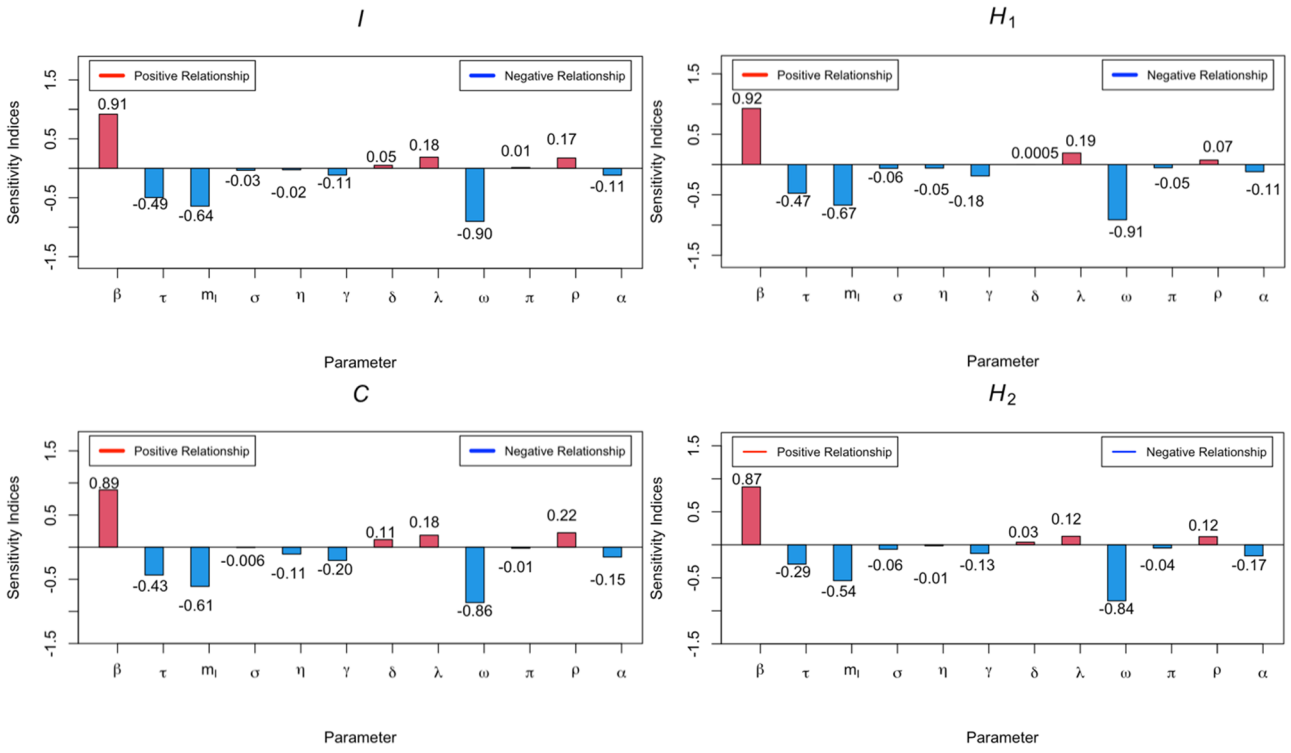

Figure 5. Sensitivity indexes table for endemic equilibrium.

5. Relationship between the basic reproduction number (R_0) and vaccination rate (τ)

In this section, we examine the influence of the vaccination rate on the spread of the epidemic by analyzing its connection with the basic reproduction number. We incrementally increase the vaccination rate within the range 0 to 0.003 and meticulously analyze its impact. Figure 6 illustrates the critical threshold representing the optimal vaccination rate necessary to effectively mitigate the epidemic spread ($R_0 = 1$). Notably, the intersection point reveals a vaccination rate of 0.0018125, corresponding to approximately 119,625 doses administered per day. This specific threshold signifies the point at which the vaccination rate achieves the pivotal status of controlling the outbreak. Therefore,

it is evident that to ensure R_0 remains below 1, a strategic vaccination approach involving the administration of at least 119,625 doses per day is imperative, particularly at the onset of the fifth wave of the COVID-19 outbreak. This underscores the significance of timely and targeted vaccination efforts in effectively curbing the spread of the epidemic:

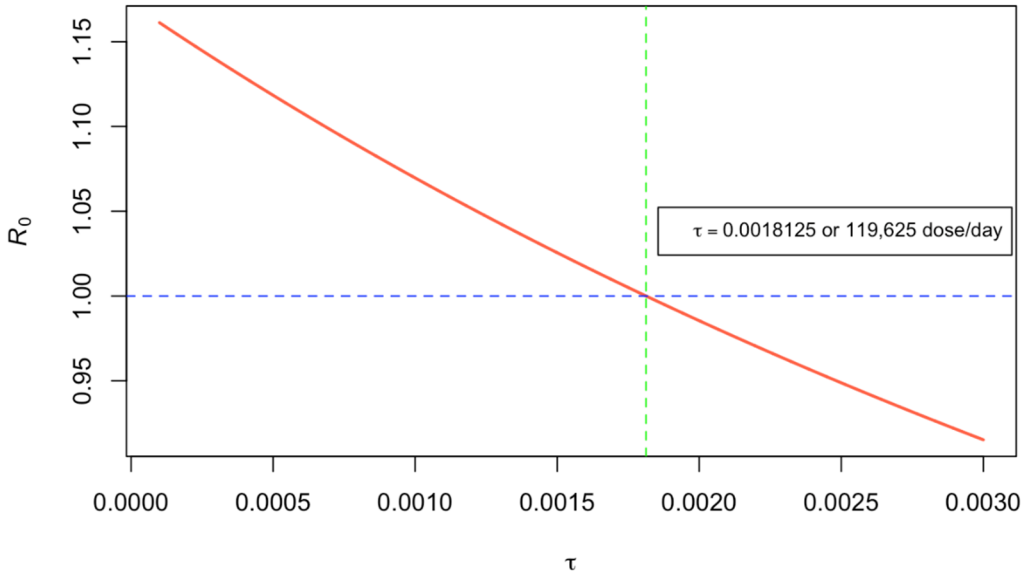

Figure 6. The optimal cutoff point for the basic reproduction number and the vaccination rate.

6. The effect of the optimal vaccination rate (119,625 doses)

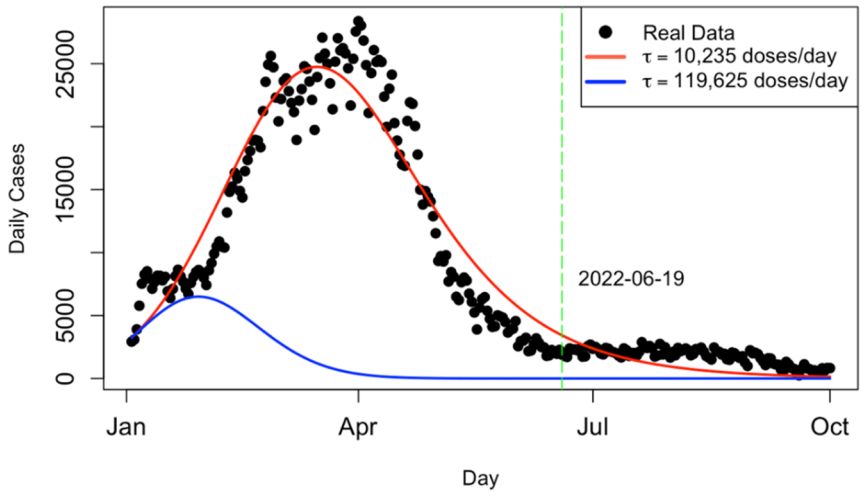

Figure 7. Comparison of two vaccination strategies: 10,235 doses/day and 119,625 doses/day.

If the susceptible population varies over time, it is preferable to use the effective reproduction number (R_t). This metric signifies the average number of secondary cases arising from an infected case at a given point during the epidemic. We compare the effective reproduction number of COVID-19 between two scenarios: the baseline, with a vaccination rate (τ) of 10,235 doses per day as of January 3, 2021, marking the beginning of the fifth-wave outbreak, and the optimal vaccination rate

(119,625 doses) identified in our simulation. Figure 7 shows that the baseline scenario reflects a trend where the number of infections begins to decline around the end of March, gradually reducing to only a few infected individuals by the end. Conversely, adopting the optimal vaccination strategy with 119,625 doses accelerates epidemic control significantly. In this scenario, infections start declining as early as the end of January, leading to complete eradication of the epidemic from the population by June 19, 2022. This intervention effectively reduces the time needed to eliminate the epidemic by 4 months.

7. Discussion

The COVID-19 pandemic, caused by severe acute respiratory syndrome coronavirus 2 (SARS-CoV-2), has posed significant challenges worldwide since its emergence in late 2019. With millions of confirmed cases and fatalities globally, understanding the dynamics of disease transmission and devising effective control strategies is paramount. In this study, we employed a comprehensive mathematical model to explore the impact of vaccination strategies on the dynamics of the pandemic, particularly in the context of Thailand.

Various studies have been conducted on COVID-19 vaccination. Intawong et al. [32] investigated the efficacy of third and fourth doses of X-ray injection in preventing COVID-19 induced by omicron strains. Their findings revealed no significant difference in protection against infection with delta and omicron strains of COVID-19 in Thailand. Aikawa et al. [33] examined the increase in immunity following administration of the vaccine's third and fourth doses. The results of this study showed that the body's immunity was not compromised by these higher dosages. Research conducted by Tartof et al. [34] and Safa et al. [35] concentrated on the third, fourth, and fifth immunization doses for individuals with compromised immune systems. Based on these assessments, it appears that vaccination should only require three doses to provide protection against COVID-19 infection in the general population. These findings emphasize the importance of booster shots in enhancing immunity and avoiding COVID-19, particularly in susceptible groups.

Our findings highlight the critical role of vaccination campaigns in mitigating the spread of COVID-19. Thailand's efforts to implement extensive vaccination drives have proven instrumental in reducing infection rates and mitigating disease severity. By analyzing real-world data and employing sophisticated mathematical modeling techniques, we elucidated the potential benefits of administering a third vaccine dose in controlling the epidemic.

One of the key insights from our study was the identification of the optimal vaccination rate necessary to effectively curb the spread of the virus. Through meticulous analysis, we determined that a vaccination rate of approximately 119,625 doses per day is pivotal in keeping the basic reproduction number (R_0) below the critical threshold of 1, thereby facilitating epidemic control. This underscores the importance of timely and targeted vaccination efforts, particularly amidst the emergence of new variants and the ongoing waves of the pandemic.

Furthermore, our study highlights the importance of considering the effectiveness of vaccination strategies in real-world scenarios. By incorporating data-driven parameter estimation techniques, we provided valuable insights into the dynamics of disease transmission and the efficacy of vaccination in preventing infections and reducing mortality rates. Our findings suggest that the administration of a third vaccine dose can significantly accelerate epidemic control and hasten the path toward eradication.

8. Conclusions

In conclusion, our study emphasized the pivotal role of vaccination campaigns in combating the COVID-19 pandemic. Through sophisticated mathematical modeling and data-driven analysis, we demonstrated the potential benefits of administering third vaccine doses in reducing infection rates and mitigating disease severity. Our findings underscore the importance of timely intervention and targeted vaccination to curb the spread of the virus and safeguard public health.

Continued research and refinement of vaccination strategies are essential to effectively navigate the evolving landscape of the pandemic. By leveraging mathematical modeling techniques and real-world data, policymakers and healthcare authorities can make informed decisions to optimize vaccination campaigns and mitigate the impact of COVID-19. Ultimately, our study contributes to the collective effort toward achieving epidemic control and safeguarding global health security in the face of emerging infectious diseases.

Use of AI tools declaration

The authors hereby declare that in preparing this document, we utilized artificial intelligence (AI)-based language processing tools to assist with grammar checking, punctuation, and overall language enhancement. The AI tools were employed solely for the purpose of language correction and did not contribute to the generation of ideas, the formulation of scientific insights, or the interpretation of data presented herein. All substantive contributions, intellectual content, and data interpretations remain our responsibility.

Acknowledgments

This research project was financially supported by Mahasarakham University 2021.

Conflict of interest

The authors declare no conflict of interest.

References

1. M. Worobey, J. I. Levy, L. M. Serrano, A. Crits-Christoph, J. E. Pekar, S. A. Goldstein, et al., The Huanan Seafood Wholesale Market in Wuhan was the early epicenter of the COVID-19 pandemic, *Science*, **377** (2022), 951–959. https://doi.org/10.1126/science.abp8715
2. World Health Organization, WHO Director-General's statement on IHR Emergency Committee on Novel Coronavirus (2019-nCoV), 2020. Available from: https://www.who.int/director-general/speeches/detail/who-director-general-s-statement-on-ihr-emergency-committee-on-novel-coronavirus-(2019-ncov).
3. P. Alam, I. Y. H. Chu, H. J. Larson, L. Lin, Social consequences of mass quarantine during epidemics: A systematic review with implications for the COVID-19 response, *J. Travel Med.*, **27** (2020), taaa192. https://doi.org/10.1093/jtm/taaa192

4. N. G. Davies, A. J. Kucharski, R. M. Eggo, A. Gimma, W. J. Edmunds, T. Jombart, et al., Effects of non-pharmaceutical interventions on COVID-19 cases, deaths, and demand for hospital services in the UK: A modelling study, *Lancet Public Health*, **5** (2020), e375–e385. https://doi.org/10.1016/S2468-2667(20)30133-X
5. H. Lau, V. Khosrawipour, P. Kocbach, A. Mikolajczyk, J. Schubert, J. Bania, et al., The positive impact of lockdown in Wuhan on containing the COVID-19 outbreak in China, *J. Travel Med.*, **27** (2020), taaa037. https://doi.org/10.1093/jtm/taaa037
6. World Health Organization, World Health Organization Coronavirus (COVID-19) Dashboard, 2022.
7. SAT-MOPH, DDC COVID-19 Interactive Dashboard 2022, 2022. Available from: https://ddc.moph.go.th/covid19-dashboard/?dashboard=main (accessed on 16 May 2023).
8. P. Jarumaneeroj, P. O. Dusadeerungsikul, T. Chotivanich, T. Nopsopon, K. Pongpirul, An epidemiology-based model for the operational allocation of COVID-19 vaccines: A case study of Thailand, *Comput. Ind. Eng.*, **167** (2022), 108031. https://doi.org/10.1016/j.cie.2022.108031
9. N. Nittayasoot, R. Suphanchaimat, P. Thammawijaya, C. Jiraphongsa, T. Siraprapasiri, K. Ploddi, et al., Real-world effectiveness of COVID-19 vaccines against severe outcomes during the period of omicron predominance in Thailand: a test-negative nationwide case–control study, *Vaccines*, **10** (2022), 2123. https://doi.org/10.3390/vaccines10122123
10. World Health Organization Country Office for Thailand, Situation of coronavirus disease 2019 in Thailand: 7 February 2024, 2024. Available from: https://www.who.int/thailand/news/detail/07-02-2024-update-on-covid-19-in-thailand--7-february-2024-THA (accessed on 4 March 2022).
11. P. Ngamchaliew, N. Kaewkuea, N. Nonthasorn, Changes in preventive behaviour after COVID-19 vaccination in Thailand: A cross-sectional study, *BMC Public Health*, **22** (2022), 2039. https://doi.org/10.1186/s12889-022-14494-x
12. World Health Organization Country Office for Thailand, Progress and Challenges in COVID-19 Vaccine Roll-Out, 2021. Available from: https://cdn.who.int/media/docs/default-source/searo/ivd/itag-2021/day2/05-thailand---progress-and-challenges-in-covid-19-vaccine-roll-out.pdf?sfvrsn=2412ff89_5 (accessed on 4 March 2023).
13. Reuters, Thailand seeks 12 mln Sinovac shots for mix-and-match vax strategy, 2021. Available from: https://www.reuters.com/world/asia-pacific/thailand-reports-daily-record-239-new-coronavirus-deaths-2021-08-17/ (accessed on 4 March 2024).
14. Department of disease control, Guidelines for people who need COVID-19 Epidemic Situation in 2021 in Thailand, 2021. Available from: https://ddc.moph.go.th/vaccine-covid19/getFiles/11/1628849610213.pdf (accessed on 15 May 2023).
15. P. Thepgumpanat, P. Wongcha-um, In First, Thailand to Mix Sinovac, AstraZeneca Vaccine Doses, Reuters, 2021. Available from: https://www.reuters.com/world/asia-pacific/thailand-starts-tighter-coronavirus-lockdown-around-capital-2021-07-12/ (accessed on 4 March 2024).
16. Hfocus, Update! Vaccination with 3 doses of vaccine "Children 12–17 years" and 4 doses stimulate immunity, 2021. Available from: https://www.hfocus.org/content/2022/03/24758 (accessed on 4 March 2024).
17. Thaipbs, The Recommended Third Dose and Fourth Dose of COVID-19 Vaccine, 2021. Available from: https://www.thaipbs.or.th/news/content/311590 (accessed on 4 March 2024).

18. Hfocus, Investigative doctor reveals the facts! Effectiveness of each brand of COVID vaccine, 2021. Available from: https://www.hfocus.org/content/2021/05/21582 (accessed on 4 March 2024).
19. C. Zimmer, J. Corum, S. L. Wee, M. Kristoffersen, Coronavirus Vaccine Tracker, 2022. Available from: https://www.nytimes.com/interactive/2020/science/coronavirus-vaccine-tracker.html (accessed on 4 March 2024).
20. K. Katella, Comparing the COVID-19 Vaccines: How Are They Different, YaleMedicine, 2023. Available from: https://www.yalemedicine.org/news/covid-19-vaccine-comparison (accessed on 4 March 2024).
21. Centers for Disease Control and Prevention, Understanding How COVID-19 Vaccines Work, 2023. Available from: https://archive.cdc.gov/www_cdc_gov/coronavirus/2019-ncov/vaccines/different-vaccines/how-they-work.html (accessed on 4 March 2024).
22. World Health Organization, What is COVID-19 vaccine efficacy, 2021. Available from: https://www.afro.who.int/news/what-covid-19-vaccine-efficacy (accessed on 4 March 2024).
23. F. Brauer, C. Castillo-Chavez, Z. Feng, Endemic disease models, in *Mathematical Models in Epidemiology*, Springer, (2019), 63–116. https://doi.org/10.1007/978-1-4939-9828-9_3
24. A. M. Salman, I. Ahmed, M. H. Mohd, M. S. Jamiluddin, M. A. Dheyab, Scenario analysis of COVID-19 transmission dynamics in Malaysia with the possibility of reinfection and limited medical resources scenarios, *Comput. Biol. Med.*, **133** (2021), 104372. https://doi.org/10.1016/j.compbiomed.2021.104372
25. K. Rajagopal, N. Hasanzadeh, F. Parastesh, I. I. Hamarash, S. Jafari, I. Hussain, A fractional-order model for the novel coronavirus (COVID-19) outbreak, *Nonlinear Dyn.*, **101** (2020), 711–718. https://doi.org/10.1007/s11071-020-05757-6
26. Q. M. Al-Mdallal, Mathematical modeling and simulation of SEIR model for COVID-19 outbreak: A case study of Trivandrum, *Front. Appl. Math. Stat.*, **9** (2023), 1124897. https://doi.org/10.3389/fams.2023.1124897
27. S. Nana-Kyere, F. A. Boateng, P. Jonathan, A. Donkor, G. K. Hoggar, B. D. Titus, et al., Global analysis and optimal control model of COVID-19, *Comput. Math. Methods Med.*, **2022** (2022), 9491847. https://doi.org/10.1155/2022/9491847
28. S. Boulaaras, R. Ramalingam, A. J. Gnanaprakasam, SEIR model for COVID-19: Stability of the standard coronavirus factor and control mechanism, *Eur. Phys. J. Spec. Top.*, **232** (2023), 2485–2495. https://doi.org/10.1140/epjs/s11734-023-00915-4
29. V. E. Papageorgiou, G. Vasiliadis, G. Tsaklidis, Analyzing the asymptotic behavior of an extended SEIR model with vaccination for COVID-19, *Mathematics*, **12** (2023), 55. https://doi.org/10.3390/math12010055
30. I. Rahimi, F. Chen, A. H. Gandomi, A review on COVID-19 forecasting models, *Neural Comput. Appl.*, **35** (2023), 23671–23681. https://doi.org/10.1007/s00521-020-05626-8
31. S. Jitsinchayakul, U. W. Humphries, A. Khan, The SQEIRP mathematical model for the COVID-19 epidemic in Thailand, *Axioms*, **12** (2023), 75. https://doi.org/10.3390/axioms12010075
32. K. Intawong, S. Chariyalertsak, K. Chalom, T. Wonghirundecha, W. Kowatcharakul, A. Thongprachum, et al., Effectiveness of heterologous third and fourth dose COVID-19 vaccine schedules for SARS-CoV-2 infection during delta and omicron predominance in Thailand: A test-negative, case-control study, *Lancet Reg. Health - Southeast Asia*, **10** (2023), 100121. https://doi.org/10.1016/j.lansea.2022.100121

33. N. E. Aikawa, L. V. Kupa, C. A. Silva, C. G. Saad, S. G. Pasoto, E. F. Yuki, et al., Strong response after fourth dose of mRNA COVID-19 vaccine in autoimmune rheumatic diseases patients with poor response to inactivated vaccine, *Rheumatology*, **62** (2023), 480–485. https://doi.org/10.1093/rheumatology/keac301
34. S. Y. Tartof, J. M. Slezak, L. Puzniak, V. Hong, T. B. Frankland, F. Xie, et al., Analysis of mRNA COVID-19 vaccine uptake among immunocompromised individuals in a large US health system, *JAMA Netw. Open*, **6** (2023), e2251833–e2251833. https://doi.org/10.1001/jamanetworkopen.2022.51833
35. K. Safa, C. N. Kotton, COVID-19 vaccines and solid organ transplantation: More doses, more protection, *Transplantation*, **107** (2023), 21–22. https://doi.org/10.1097/TP.0000000000004387
36. K. Bardosh, A. Krug, E. Jamrozik, T. Lemmens, S. Keshavjee, V. Prasad, et al., COVID-19 vaccine boosters for young adults: A risk benefit assessment and ethical analysis of mandate policies at universities, *J. Med. Ethics*, **50** (2024), 126–138. https://doi.org/10.1136/jme-2022-108852
37. S. Ramot, O. Tal, Attitudes of healthcare workers in Israel towards the fourth dose of COVID-19 vaccine, *Vaccines*, **11** (2023), 385. https://doi.org/10.3390/vaccines11020385
38. M. H. DarAssi, T. A. Shatnawi, M. A. Safi, Mathematical analysis of a MERS-Cov coronavirus model, *Demonstr. Math.*, **55** (2022), 265–276. https://doi.org/10.1515/dema-2022-0022
39. T. Theparod, P. Kreabkhontho, W. Teparos, Booster dose vaccination and dynamics of COVID-19 pandemic in the fifth wave: An efficient and simple mathematical model for disease progression, *Vaccines*, **11** (2023), 589. https://doi.org/10.3390/vaccines11030589
40. T. Patalon, Y. Saciuk, A. Peretz, G. Perez, Y. Lurie, Y. Maor, et al., Waning effectiveness of the third dose of the BNT162b2 mRNA COVID-19 vaccine, *Nat. Commun.*, **13** (2022), 3203. https://doi.org/10.1038/s41467-022-30884-6
41. Centers for Disease Control and Prevention, COVID-19 Vaccine Effectiveness Update, 2022. Available from: https://covid.cdc.gov/covid-data-tracker/#vaccine-effectiveness (accessed on 23 July 2023).
42. World Health Organization Country Office for Thailand, COVID-19 Situation, Thailand 27 July 2022, 2022. Available from: https://cdn.who.int/media/docs/default-source/searo/thailand/2022_07_27_tha-sitrep-243-covid-19.pdf?sfvrsn=23bab9e2_1 (accessed on 23 July 2023).
43. BBC NEWS Thailand, Sinovac-Sinopharm: COVID-19 evaluating the two Chinese vaccinations that Thailand uses and their respective efficacies, 2021. Available from: https://www.bbc.com/thai/thailand-57525497 (accessed on 15 March 2024).
44. Ministry of Higher Education Science Research and Innovation, 100 million doses, COVID-19 vaccination statistics in Thailand, 2021. Available from: https://www.mhesi.go.th/index.php/all-media/infographic/5379-6412221Covid_19.html (accessed on 14 March 2024).
45. K. Dietz, The estimation of the basic reproduction number for infectious diseases, *Stat. Methods Med. Res.*, **2** (1993), 23–41. https://doi.org/10.1177/096228029300200103
46. The Bureau of Registration Administration, Official population statistics from the civil registration (monthly), 2022. Available from: https://stat.bora.dopa.go.th/stat/statnew/statMONTH/statmonth/#/displayData (accessed on 15 May 2023).

47. Department of Health Ministry of Public Health, Report on progress of COVID-19 vaccination services, 2022. Available from: https://public.tableau.com/views/SATCOVIDDashboard/1-dash-tiles?:showVizHome=no (accessed on 14 March 2024).
48. UK Health Security Agency, SARS-CoV-2 variants of concern and variants under investigation in England, 2022. Available from: https://assets.publishing.service.gov.uk/government/uploads/system/uploads/attachment_data/file/1050236/technical-briefing-34-14-january-2022.pdf (accessed on 19 May 2023).
49. Z. Zi, Sensitivity analysis approaches applied to systems biology models, *IET Syst. Biol.*, **5** (2011), 336–346. https://doi.org/10.1049/iet-syb.2011.0015